Parameter Characterization of Drying of Porous Spherical Particles

James L. Manganaro
New Jersey Center for Microchemical Systems
Stevens Institute of Technology
Hoboken, NJ 07030
email: JLJM1@rcn.com

Abstract

A quasi-steady state shell and shrinking core model which recognizes heat and mass transfer resistances in both the gas and particle phases for drying of a porous particle is proposed. This model when embedded in a spreadsheet combined with a genetic algorithm for parameter identification provides an easy means of characterizing the drying process. In drying, four major parameters are typically unknown, two related to the process, heat and mass transfer coefficients, and two which incorporate porous particle properties, shell thermal conductivity and vapor diffusivity. It is shown how these 4 parameters may be determined from experimental drying data. If the ratio between heat and mass transfer coefficient can be assumed constant then the number of characterizing parameters reduces to only three. When $Nu_{IN}/Sh_{IN} > 1.0$, mass mobility is relatively greater than thermal transport in the shell and it is shown that this condition leads to unexpected behavior in which temperature at the wet core is predicted to decrease with time while surface temperature of the particle increases with time. The model was applied to literature data for drying rice. For this particular case, although moisture diffusion within the particle is important external heat transfer was found to be the controlling mode.

Introduction

The drying of porous particulate material by a gas is governed by process parameters and particle properties. Process parameters include gas temperature, partial pressure of solvent in the gas phase, and particle heat and mass transfer coefficients. The term "solvent" is used in the sense of evaporating species. Particle properties include thermal conductivity, diffusivity within the particle, heat of vaporization (in the broadest sense), and size of the particle. This paper presents a simple method of parametatizing the drying process within the assumptions of the model.

In a previous paper by the author [1], equations were developed governing the dehydration of a spherical particle. Transport of heat (by conduction) and mass (by vapor diffusion) through the porous shell were taken into account. However, in ref. [1] the equation describing heat transport in the particle considered only conduction. Convective heat transport due to the diffusion of cooler solvent vapor away from the wet core and through the porous shell was neglected. In this paper the scope of the heat transport equation is broadened to include convective heat transfer. Indeed it was found that, if the convective heat transfer term is neglected, an unreasonably small shell thermal conductivity would have to be postulated in order to match the actual drying data. The model presented here allows for heat and mass transfer resistances in both the gas particle phases.

At the time the equations were formulated in 1980, their solution required codes such as FORTRAN and BASIC. Subsequent development in spreadsheets and parameter identification tools has now allowed much more tractable solution as well as greater power in parameter identification. A modification of the equations of [1] are adopted here to spreadsheet solution and

applied as a means of characterizing the drying process for particulate solids from experimental drying data. The software that was used for parameter identification was Evolver© 4.0 (a product of Palisade Corp., Ithaca, NY). Evolver© uses a genetic algorithm for determining optimum parameter values and may be incorporated into Excel as an add-in.

It is anticipated that the model should be applicable to dryers such as fluid bed, spouted bed, vibrating fluid bed and possible rotary. The speed of drying that occurs in flash and spray dryers makes the validity of the quasi-steady state assumption problematic for this kind of equipment.

Model

The shell and shrinking core model along with some of the variables is shown in Figure 1. The gas phase transfers heat to the outer surface of the particle and is conducted through the shell of completely dried material to the wet core where solvent evaporates and diffuses through the porous shell. The solvent in diffusing through the shell represents a convective heat flow. The region with which we are concerned is the shell.

Figure 1 Shell and Shrinking Core Model

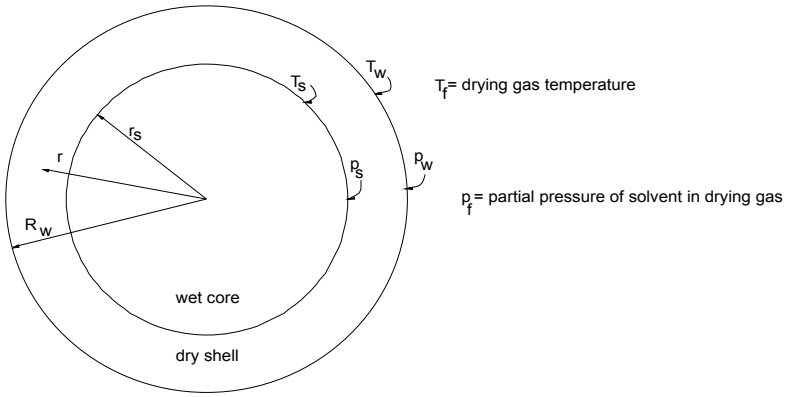

Shell and Shrinking Core Model of Particle

Base Case

To study the model behavior we take a theoretical base case to which we can compare the effect of parameter deviations. For the base case, consider water evaporating from a porous spherical particle in a fluid bed where air is the drying gas. It is assumed that the drying gas temperature and partial pressure of water surrounding the particle remain constant with time. This is not a necessary assumption as the treatment can be extended to the case where drying gas temperature and humidity vary with time as will be seen later. The time history of a single particle will be followed. The typically known parameters are taken to be:

Particle diameter = 3 mm
T_f = 200 F
p_f = 0.03 atm (of water)
ΔH = 18,772 BTU/lb-mol H2O
ρ^* = 1.56 lb-mol H2O/ft^3

For purposes of illustrating model behavior we determine what might be reasonable values for h, k_G, Nu_{IN}, and Sh_{IN}. In the water-air system, Trybal (p. 194 of ref. [2]) suggests that the psychometric ratio, h/k_Y, is equal to 0.227. This can be converted to the units used in this paper by $h/k_G = 28.8(h/k_Y)$. Hence, for our case

$$h/k_G = 6.54 \text{ BTU-atm/lbmol H2O-}^oF \qquad (1.1)$$

Consider the following hypothetical values: h = 6.9 BTU/h-ft^2-/F and k_G = 1.06 lbmol H2O/h-ft^2-atm, Nu_{IN} = 0.132 and Sh_{IN} = 123.4.

The Excel © spreadsheet with input and output for the base case is shown in Table 1. This table reports T_s, T_w, p_s, p_w, and the extent of dryness expressed in several ways as a function of drying time.

Table 1 Spreadsheet Input and Output

Base Case											
Particle dia, mm				3		Particle radius, ft					0.004921
Temp of drying gas, F				200			Rw^3				1.19E-07
Partial pressure of water vapor in drying gas, atm				0.03		lambda star					6.08E-05
c1 vapor press equ				18.3486		Estimate of internal Diff coef, ft^2/h					0.020278
c2 vapor press equ				3851.22							
c3 vapor press equ				228.7							
Heat of vaporization, BTU/lb-mol H2O				18772							
Initial molar water density, lbmol H2O/ft^3				1.560							
Initial density of particle, lb/ft^3				75.00							
h, BTU/h-ft^2-F				**6.90**							
Kg, lb-mol H2O/h-ft^2-atm H2O				**1.06**							
Nu_{IN}				**0.132**							
Sh_{IN}				**123.40**							
Time step, h				0.01							
heat capacity of solvent vapor, BTU/lb-F				0.48							
molecular weight of solvent				18							
h/kg, BTU-atm H2O/(lbmol H2O-F)				6.54							
Constant c4, DeltaH*KG/h units=F/atm				2870							
Constant A, ft^3/h-F				5.71E-09							
Consant B, atm/F				3.48E-04							
Constant c5 = A/Rw ^3, 1/h-F				0.04788							
Estimate of internal k, BTU/h-ft-F				0.2572					w t solvent per		
Time	pf(t)	Tf(t)							predicted	per w t of	wt%
min	atm	F	Zeta s	x	Ts, F	ps, atm	Tw, F	pw, atm	% Dried	dry solids	solvent
0.00	0.0300	200	1.00	0.000	100.0	0.0648	100.0	0.065	0.0	0.598	37.4
0.60	0.0300	200	0.9521	0.050	137.7	0.1854	138.1	0.052	13.7	0.517	34.1
1.20	0.0300	200	0.9194	0.088	148.0	0.2414	148.6	0.048	22.3	0.465	31.7
1.80	0.0300	200	0.8903	0.123	154.5	0.2828	155.2	0.046	29.4	0.422	29.7
2.40	0.0300	200	0.8633	0.158	159.1	0.3164	160.0	0.044	35.7	0.385	27.8
3.00	0.0300	200	0.8376	0.194	162.8	0.3451	163.7	0.043	41.2	0.352	26.0
3.60	0.0300	200	0.8128	0.230	165.8	0.3702	166.8	0.042	46.3	0.321	24.3
4.20	0.0300	200	0.7888	0.268	168.3	0.3927	169.4	0.041	50.9	0.294	22.7
4.80	0.0300	200	0.7652	0.307	170.6	0.4132	171.7	0.040	55.2	0.268	21.1
5.40	0.0300	200	0.7421	0.348	172.5	0.4320	173.7	0.039	59.1	0.245	19.7
6.00	0.0300	200	0.7192	0.390	174.3	0.4495	175.5	0.039	62.8	0.223	18.2
6.60	0.0300	200	0.6966	0.436	175.8	0.4658	177.2	0.038	66.2	0.202	16.8
7.20	0.0300	200	0.6740	0.484	177.3	0.4812	178.7	0.037	69.4	0.183	15.5
7.80	0.0300	200	0.6515	0.535	178.6	0.4959	180.0	0.037	72.3	0.166	14.2
8.40	0.0300	200	0.6290	0.590	179.9	0.5098	181.3	0.037	75.1	0.149	13.0
9.00	0.0300	200	0.6064	0.649	181.0	0.5231	182.5	0.036	77.7	0.133	11.8
9.60	0.0300	200	0.5837	0.713	182.1	0.5359	183.7	0.036	80.1	0.119	10.6
10.20	0.0300	200	0.5608	0.783	183.2	0.5483	184.8	0.035	82.4	0.106	9.5
10.80	0.0300	200	0.5376	0.860	184.2	0.5603	185.8	0.035	84.5	0.093	8.5

Behavior Predicted by the Model

Model behavior was studied by using the base parameters of Table 1 onto which is superimposed several combinations of the four controlling parameters (h, k_G, Nu_{IN}, and Sh_{IN}), specifically

- effect of low heat and mass transfer coefficients (low h and k_G)
- effect of low internal thermal conductivity (large Nu_{IN})
- effect of low internal mass diffusivity (large Sh_{IN})
- effect of $Nu_{IN}/Sh_{IN} > 1.0$

Calculated output is shown in Figure 2a through 2e for a 3 mm diameter particle. Figure 2a plots the base case calculated output. In Figure 2b, the heat and mass transfer coefficients, h and k_G, are low relative to the base case. It is seen that drying rate is uniformly reduced relative to the base case with no abrupt change in rate. Wall and core temperatures (T_w and T_s) remain close together for the relatively high thermal conductivity. A strong partial pressure gradient is indicated.

In Figure 2c the effect of low shell thermal conductivity relative to the base case as evidenced by a high Nu_{IN} is examined. In this case the drying curve exhibits a slight knee where the drying rate rapidly falls off at an early stage in the drying. This is due to the enhanced insulating nature of the shell compared to the base case. Note also in Figure 2c that the wall and core temperatures (T_w and T_s) become separated by 40 – 50 F.

In Figure 2d, low internal diffusion coefficient as indicated by high Sh_{IN}, is explored. There is again an abrupt change in drying rate (a knee) which was also characteristic of the low thermal conductivity case (Figure 2c). This is due to the build up shell thickness resulting in a relatively impermeable layer which impedes further drying. In this case the wall and core temperatures remain close together.

In the cases considered above (Figures 2a through 2d) the ratio Nu_{IN}/Sh_{IN} was <1.0 with the result that the calculated core temperature, T_s, increased with time. This is normally expected. However, when $Nu_{IN}/Sh_{IN} > 1.0$, symptomatic of better internal mass transfer as compared to internal heat transport, we see in Figure 2e that the core temperature, T_s, actually decreases with drying time even as the outer surface temperature, T_w, increases with time. This is due to the greater thermal insulation of the shell compared to its mass diffusivity. This situation might possibly occur in the drying of, for example, aerogels which have very low thermal conductivity but might support a reasonably high mass diffusivity.

The temperature and partial pressure profiles can be estimated. Consider the base case in which the drying time has reached 10.8 minutes and the reduced radius of the core has been brought to a value of $\zeta s = 0.54$ (i.e., $1-\zeta_s^3 = 84\%$ of the particle has been dried). For this case with $\zeta_s = 0.54$, we have $T_s = 184.2$ F and $p_s = 0.56$ atm (see Table 1), where ζ varies within the shell inclusively between 0.54 and 1.0. For this situation the temperature and water vapor concentration profiles are calculated to be as shown in Figure 3. Note that the temperature

Figure 2 Base Case and Variations

a.

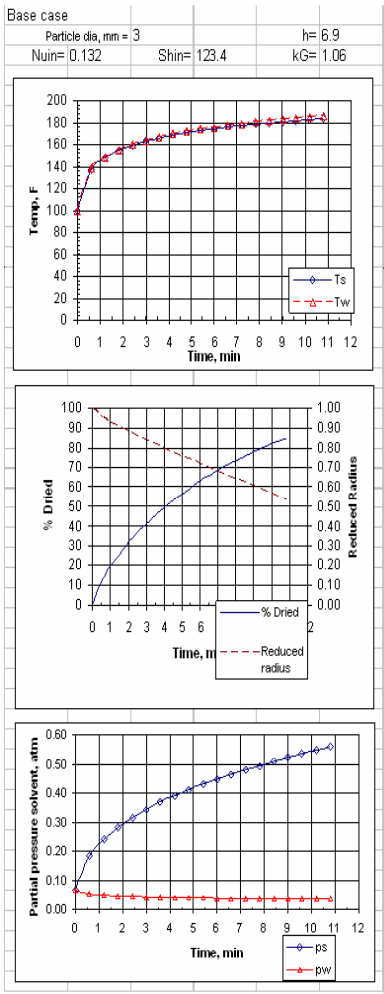

b.

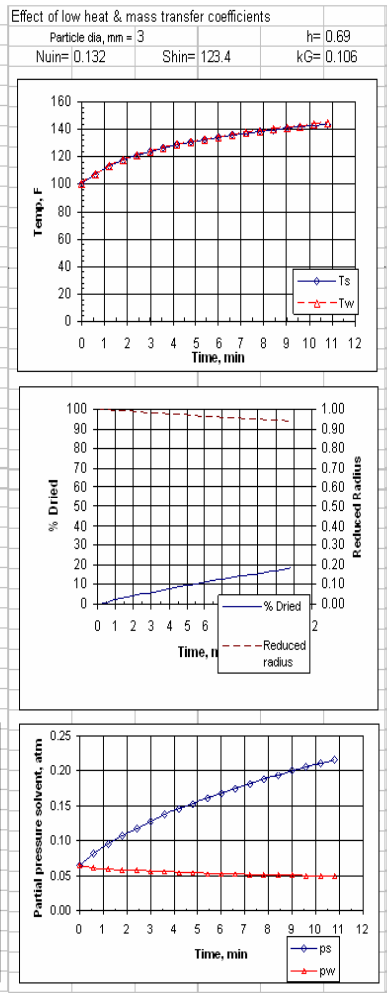

c.

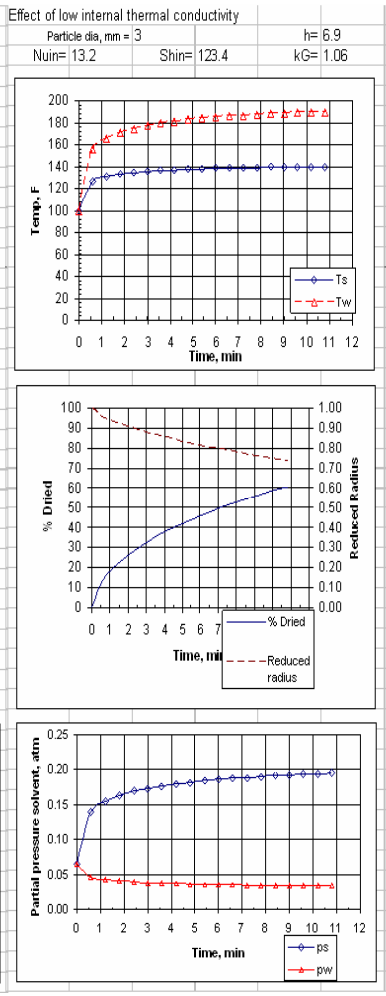

d.

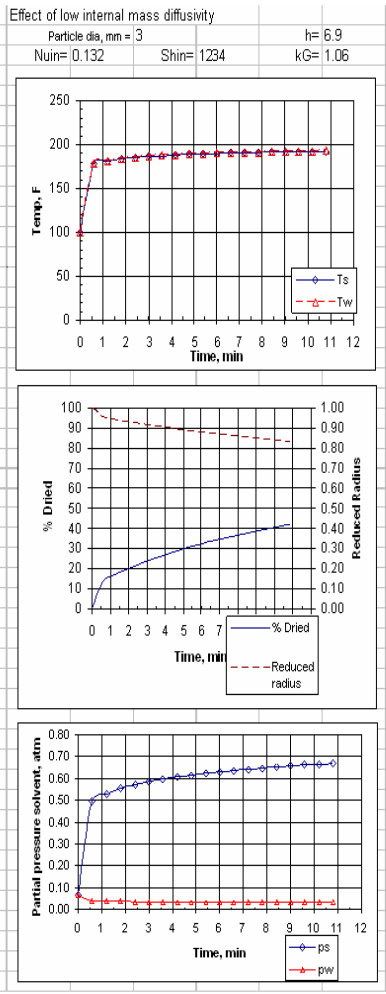

e.

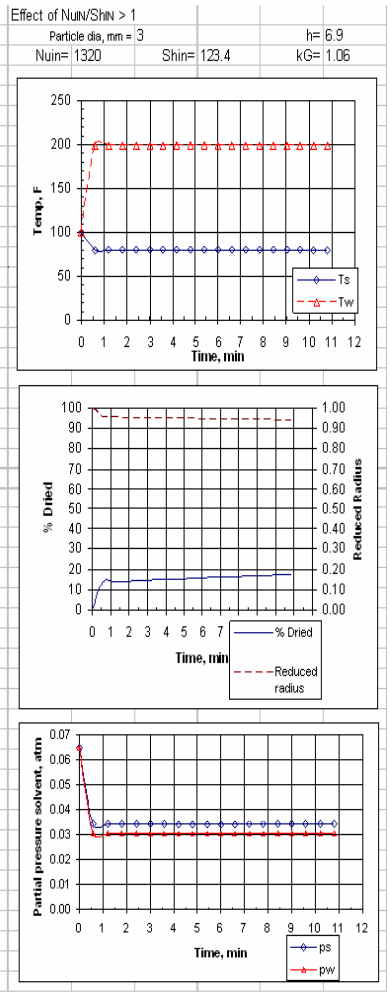

profile is relatively flat but the water vapor concentration is rather significant and achieves considerable pressure (over 0.5 atm) at the core for the parameters chosen. Interestingly, the temperature profile, although rather flat, is concave downward while the vapor pressure profile is concave upward.

Figure 3 Temperature and Water Vapor Concentration Profiles in the Shell

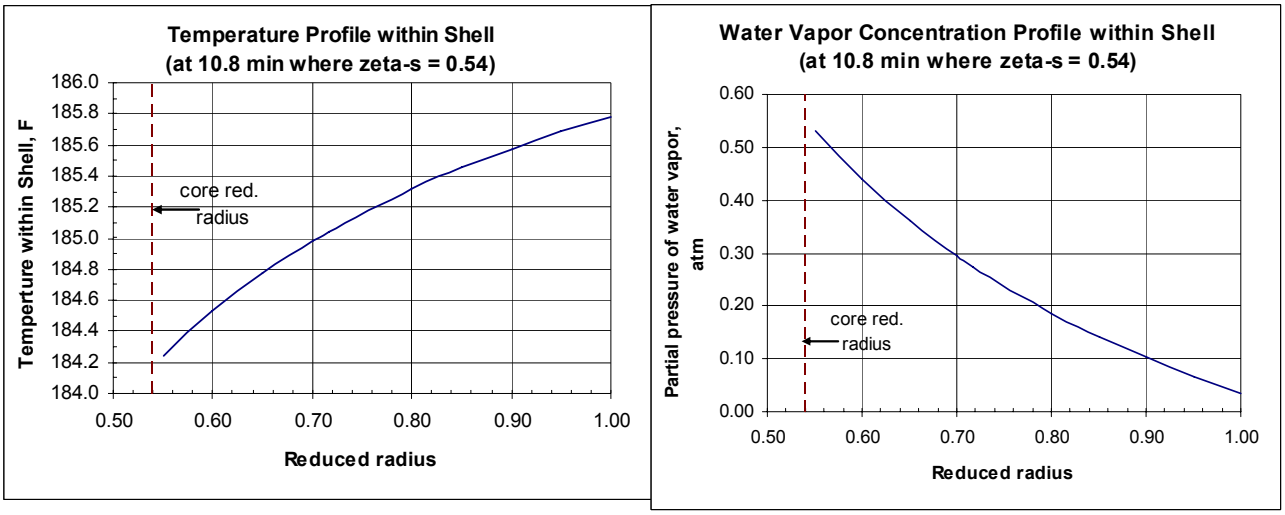

Parameter Identification: Application to Spouted Bed Drying of Rice

Precious little complete drying data is reported in the open literature which can be compared with predictions of a model. However, Zahed and Epstein [3] theoretically treat spouted bed drying of rice in which batch data reported by Zuritz and Singh [4] are referenced in a comprehensive fashion. Their analysis assumes that the mass transfer within the particle dominates drying of the particle. As will be seen, the parameters identified by the shell and core model appear to indicate that although diffusion through the particle is important, external heat transfer may have the greatest effect.

A spouted bed can be viewed as well mixed and comparable to a fluid bed. It is the data given in Zahed and Epstein [3] for the batch drying of rough rice to which we will apply the present model. The drying data is found the Tables 4 and 5 of ref. [3] for 52 C inlet air for two inlet air temperatures, 52.0 C and 70.2 C. The data for the 52.0 C inlet air temperature was used to determine optimum parameter values. These parameters were then applied in predicting the 70.2 C case and found to agree well with the experimental data. The drying data reported in [3] is for a time period of 35 minutes in which the moisture content of the rice is reduced from 0.3565 lb/lb to 0.2895 lb/lb. In order to use our model we need to know the exit gas temperature and humidity (T_f and p_f). It was assumed that the external heat and mass transfer coefficients are linked by eq. (1.1) so that we need to identify only h, Nu_{IN} and Sh_{IN} that will best fit the data.

After allowing Evolver to identify the best values of h, Nu_{IN} and Sh_{IN} to fit the moisture content of the rice, the results of Table 2 for the 52 C inlet air case are obtained. A plot of the actual data for the moisture content of the solids is shown in Figure 4. The thermal conductivity of the shell is

estimated to be 0.013 BTU/h-ft-F which is small and on the order of air. The diffusivity within the shell is estimated to 0.0022 ft^2/h which is about one-four hundredth that of water in air.

A plot of the shell and core predicted rice wall temperature versus time is shown in Figure 5 along with the exit air temperature and the predictions of [3]. Zahed and Epstein note that the surface temperature of the grain is expected to lag the air temperature so that the thermocouple gives some intermediate value between the air and the grain surface. In a subsequent paper [5] they find an improvement in predicting both the grain moisture and also the surface temperature if diffusivity is estimated not on the basis of moisture content at the grain surface but averaged through out the particle and giving rise to the concept of "a receding vapor-liquid interface within the grain." The shell and core model gives a better fit to the grain surface temperature at early time but less agreement at longer times. However, the shape of the predicted surface temperature from shell and core model is reasonable. Figure 6 gives the predicted temperature and vapor pressure profiles within the rice particle.

Table 2 Parameter Identification for the Data of Zahed and Epstein, ref. [3]

Particle dia, mm	3.692	Particle radius, ft	0.006056
Temp of drying gas, F	125.6	Rw^3, ft^3	2.22E-07
Partial pressure of water vapor in drying gas, atr	0.009500	lambda star	0.000181
c1 (see eq 29)	18.3486	Estimate of internal Diff coef, ft^2/h	0.002184
c2 (see eq 29)	3851.22		
c3 (see eq 29)	228.7		
Heat of vaporization, BTU/lb-mol H2O	20160		
Initial molar water density, lbmol H2O/ft^3	1.095		
Initial density of particle, lb/ft^3	75.00		
h, BTU/h-ft^2-F	**0.90**		
Kg, lb-mol H2O/h-ft^2-atm H2O	**0.14**		
Nu_{IN}	**0.42**		
Sh_{IN}	**164.06**		
Time step, h	0.0125		
heat capacity of solvent vapor, BTU/lb-F	0.48		
molecular weight of solvent	18		
h/k_g, BTU-atm H2O/(lbmol H2O-F)	6.54		
Constant c4, DeltaH*K_G/h units=F/atm	3083		
Constant A, ft^3/h-F	1.50E-09		
Consant B, atm/F	3.24E-04		
Constant c5 = A/R_w^3, 1/h-F	0.00677		
Estimate of internal k, BTU/h-ft-F	0.0130037		

Time min	pf(t) atm	Tf(t) F	Zeta s	Ts, F	ps, atm	Tw, F	pw, atm	predicted % Dried	predicted wt solvent per wt of dry solids	wt% solvent	measured wt solvent per wt of dry solids	% dev from meas deviation
0.00	0.0169	100	1.00	71.6	0.0261	71.6	0.03	0.0	0.356	26.3	0.3573	0.058
1.50	0.0167	101	0.995	76.3	0.0305	76.3	0.02	1.4	0.352	26.0	0.353	0.262
3.00	0.0165	101	0.991	79.2	0.0337	79.3	0.02	2.6	0.347	25.8	0.350	0.397
4.50	0.0162	102	0.988	81.5	0.0362	81.6	0.02	3.7	0.343	25.6	0.346	0.440
6.00	0.0160	102	0.984	83.2	0.0384	83.4	0.02	4.7	0.340	25.4	0.342	0.415
7.50	0.0158	103	0.981	84.8	0.0403	84.9	0.02	5.6	0.336	25.2	0.338	0.348
9.00	0.0156	104	0.978	86.1	0.0421	86.3	0.02	6.5	0.333	25.0	0.335	0.265
10.50	0.0154	104	0.975	87.3	0.0437	87.5	0.02	7.4	0.330	24.8	0.332	0.182
12.00	0.0152	105	0.972	88.4	0.0453	88.6	0.02	8.2	0.327	24.7	0.328	0.110
13.50	0.0150	105	0.969	89.5	0.0468	89.7	0.02	9.0	0.324	24.5	0.325	0.055
15.00	0.0148	106	0.966	90.4	0.0483	90.7	0.02	9.8	0.321	24.3	0.322	0.020
16.50	0.0146	107	0.963	91.4	0.0497	91.6	0.02	10.6	0.319	24.2	0.319	0.003
18.00	0.0144	107	0.961	92.2	0.0511	92.5	0.02	11.3	0.316	24.0	0.316	0.001
19.50	0.0142	108	0.958	93.1	0.0524	93.3	0.02	12.1	0.313	23.9	0.313	0.008
21.00	0.0140	108	0.955	93.9	0.0538	94.2	0.02	12.8	0.311	23.7	0.310	0.021
22.50	0.0138	109	0.953	94.7	0.0551	95.0	0.02	13.5	0.308	23.6	0.308	0.033
24.00	0.0136	110	0.950	95.5	0.0564	95.8	0.02	14.2	0.306	23.4	0.305	0.040
25.50	0.0133	110	0.948	96.2	0.0577	96.5	0.02	14.9	0.303	23.3	0.303	0.040
27.00	0.0131	111	0.945	97.0	0.0591	97.3	0.02	15.6	0.301	23.1	0.300	0.032
28.50	0.0129	111	0.942	97.7	0.0604	98.0	0.02	16.3	0.298	23.0	0.298	0.018

Figure 4 Moisture Content of Solids (52 C inlet air)

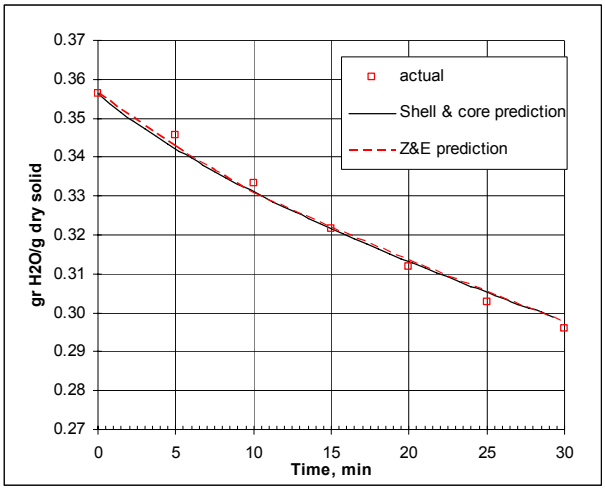

Figure 5 Predicted Particle Wall Temperature (52 C inlet air)

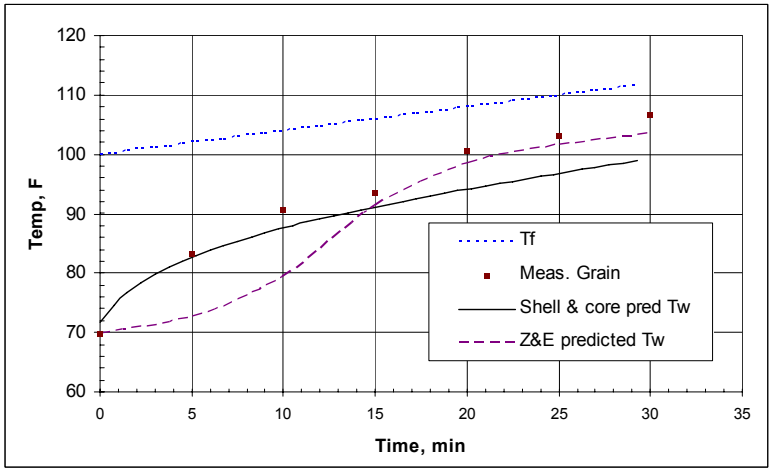

Figure 6 Calculated Temperature and Vapor Pressure Profiles within Shell (52 C inlet air)

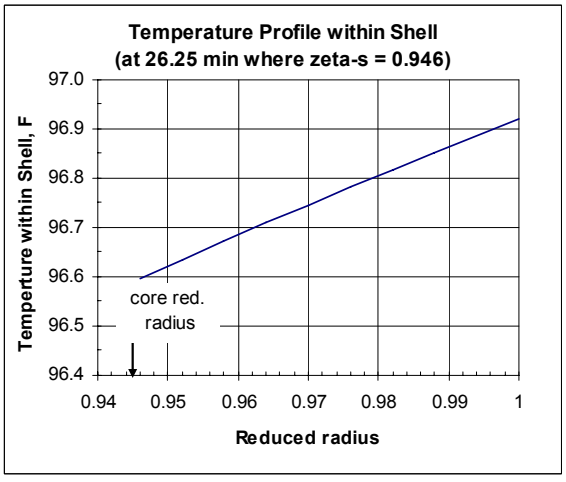

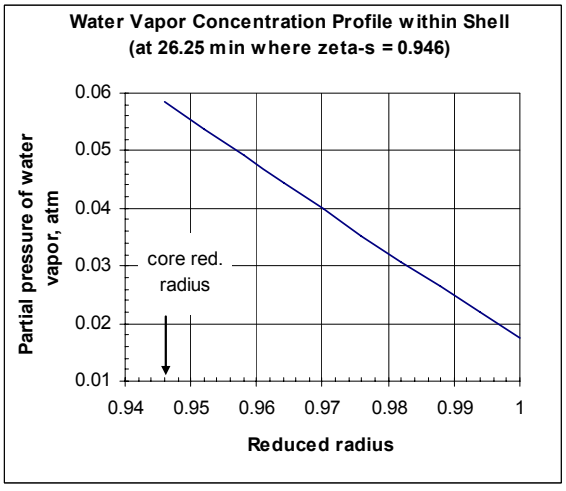

Conclusions

The approach and spreadsheet developed here can provide a useful practical tool for the analysis of drying rate data from which characterization can be made of drying equipment effectiveness and particle properties. It is recommended that this approach be further tested against existing data sets to better understand its value and limitations and what modifications might be needed to accommodate less restrictive assumptions.

Acknowledgement

The author is indebted to Prof. Owen T. Hanna (UC Santa Barbara) for his helpful comments on the analysis and to Prof. Norman Epstein (U. of British Columbia) for his insight on understanding the data relative to model.

References

1. Manganaro, J., *Heat and mass transfer in particle dehydration.* Ind. Eng. Chem Prod. Res. Dev., 1980. 19(no. 4): p. 617-622.
2. Trybal, R.E., *Mass Transfer Operations*. 2nd ed. 1968: McGraw Hill.
3. Zahed, A.H., N. Epstein, *Batch and continuous spouted bed drying of ceral grains: the thermal equilibrium model.* Canadian J. of Chem. Eng., 1992. 70: p. 945.
4. Zuritz, C.A., R.P. Singh, *Simulation of rough rice drying in a spouted-bed*, in *Drying '82*, A.S. Munjumdar, Editor. 1982, McGraw Hill Hemisphere: New York. p. 239-247.
5. Zahed, A.H., N. Epstein, *On the diffusion mechanism during spouted bed drying of cereal grains.* Drying Technology, 1993. 11(2): p. 401.